AMERICAN SOCIETY FOR MICROBIOLOGY | Journal of Bacteriology®

RESEARCH ARTICLE

Lon Protease Removes Excess Signal Recognition Particle Protein in *Escherichia coli*

Beate Sauerbrei,[a] Jan Arends,[a] Danja Schünemann,[b] Franz Narberhaus[a]

[a]Microbial Biology, Ruhr University Bochum, Bochum, Germany
[b]Molecular Biology of Plant Organelles, Ruhr University Bochum, Bochum, Germany

ABSTRACT Correct targeting of membrane proteins is essential for membrane integrity, cell physiology, and viability. Cotranslational targeting depends on the universally conserved signal recognition particle (SRP), which is a ribonucleoprotein complex comprised of the protein component Ffh and the 4.5S RNA in *Escherichia coli*. About 25 years ago it was reported that Ffh is an unstable protein, but the underlying mechanism has never been explored. Here, we show that Lon is the primary protease responsible for adjusting the cellular Ffh level. When overproduced, Ffh is particularly prone to degradation during transition from exponential to stationary growth and the cellular Ffh amount is lowest in stationary phase. The Ffh protein consists of two domains, the NG domain, responsible for GTP hydrolysis and docking to the membrane receptor FtsY, and the RNA-binding M domain. We find that the NG domain alone is stable, whereas the isolated M domain is degraded. Consistent with the importance of Lon in this process, the M domain confers synthetic lethality to the *lon* mutant. The Ffh homolog from the model plant *Arabidopsis thaliana*, which forms a protein-protein complex rather than a protein-RNA complex, is stable, suggesting that the RNA-binding ability residing in the M domain of *E. coli* Ffh is important for proteolysis. Our results support a model in which excess Ffh not bound to 4.5S RNA is subjected to proteolysis until an appropriate Ffh concentration is reached. The differential proteolysis adjusts Ffh levels to the cellular demand and maintains cotranslational protein transport and membrane integrity.

IMPORTANCE Since one-third of all bacterial proteins reside outside the cytoplasm, protein targeting to the appropriate address is an essential process. Cotranslational targeting to the membrane relies on the signal recognition particle (SRP), which is a protein-RNA complex in bacteria. We report that the protein component Ffh is a substrate of the Lon protease. Regulated proteolysis of Ffh provides a simple mechanism to adjust the concentration of the essential protein to the cellular demand. This is important because elevated or depleted SRP levels negatively impact protein targeting and bacterial fitness.

KEYWORDS proteolysis, SRP, protein targeting, heat shock protein, Lon protease, heat shock

Bacteria employ several protein transport systems in parallel to target a large amount of extracytoplasmic proteins to their appropriate destinations (1). Cotranslational targeting of nascent proteins to the membrane has the advantage of protecting the growing polypeptide chain from misfolding and aggregation while it travels from the cytoplasm to the membrane. A key component of cotranslational targeting is the signal recognition particle (SRP), which is found in all domains of life (2, 3). In bacteria, it is a ribonucleoprotein composed of the universally conserved protein component Ffh (fifty-four-homolog) and an RNA component, such as the 4.5S RNA in *Escherichia coli*. Ffh contains two functional domains, the NG domain at the N-terminal end that is

Citation Sauerbrei B, Arends J, Schünemann D, Narberhaus F. 2020. Lon protease removes excess signal recognition particle protein in *Escherichia coli*. J Bacteriol 202:e00161-20. https://doi.org/10.1128/JB.00161-20.

Editor Ann M. Stock, Rutgers University-Robert Wood Johnson Medical School

Address correspondence to Franz Narberhaus, franz.narberhaus@rub.de.

Received 26 March 2020
Accepted 15 April 2020
Accepted manuscript posted online 4 May 2020
Published 25 June 2020

followed by the M domain. The methionine-rich M domain recognizes the signal peptide of the nascent polypeptide emerging from the ribosome and interacts with the RNA component. The NG domain has an intrinsic GTPase activity and interacts with the homologous NG domain of the membrane receptor called FtsY. The 4.5S RNA accelerates SRP/FtsY complex formation and stimulates the GTPase activity of the complex, which results in dissociation of the complex and release of the nascent chain to the translocon machinery in the bacterial membrane (3, 4).

The SRP composition has undergone profound changes during evolution. In most cases it is a ribonucleoprotein, although the size and composition of the complex varies widely across species. A remarkable exception is the chloroplast SRP (cpSRP) of higher plants, for example in the model plant *Arabidopsis thaliana*. The M domain of the Ffh homolog cpSRP54 lost RNA-binding ability and an RNA component is absent in *Arabidopsis* (5–7). Instead, cpSRP54 acts as protein-only particle and exists in two distinct pools with different functionalities. Associated with ribosomes, it mediates cotranslational targeting of central plastid-encoded photosynthetic proteins to the thylakoid membrane. In complex with the chloroplast-specific cpSRP43 protein, it is responsible for posttranslational targeting of nuclear-encoded light harvesting proteins (8, 9). Evolutionary intermediate SRP variants exist in chloroplasts of lower plants, for example in the moss *Physcomitrella patens*. This species contains cpSRP43 as well as an RNA component with a large apical loop and relatively weak affinity for cpSRP54 (8, 10).

A principle limitation of cotranslational protein targeting is the slow translation rate of the ribosome and the low concentration of the secretion machinery involved (4, 11). In comparison to the ribosomes, the SRP complex is largely stoichiometrically underrepresented. In *E. coli*, there are roughly one Ffh and four 4.5S RNA molecules per 100 ribosomes (12, 13). To maintain efficient protein targeting, it is therefore crucial that free SRP complexes rapidly reassociate with translating ribosomes. Although the number of SRP particles seems critically low, even lower levels can be tolerated (14, 15). After 2 h of depletion of *ffh* expression, cells still contained a considerable amount of SRP and the Ffh levels were kept at about 1% of the amount in control cells even after prolonged depletion (16). This finding suggested homeostatic control mechanisms that operate to maintain a certain threshold of SRP in the cell. Among the consequences of SRP depletion is the slowdown of membrane protein biogenesis, as well as protein misfolding and aggregation accompanied by the induction of the heat shock response (15, 16). Interestingly, an excess of Ffh can also be deleterious because it selectively inhibits the expression of membrane proteins (17). All these results suggest that cells balance the amount of SRP by removing surplus Ffh on the one hand and by maintaining a critical level of this essential protein on the other hand. It is thus not surprising that it was reported a long time ago that free Ffh is prone to proteolysis with a half-life of about 20 min (12). The question of which protease is responsible for Ffh turnover has never been addressed and this information gap was the motivation of our study.

There are five ATP-fueled proteases in *E. coli*, namely, FtsH, Lon, ClpAP, ClpXP, and HslUV, which have numerous functions in protein quality control and regulated proteolysis (18–21). FtsH is a membrane-anchored protease (22). It is the only essential protease in *E. coli* due to its regulatory function in lipopolysaccharide (LPS) biosynthesis (23). The remaining proteases are cytoplasmic. Lon is responsible for clearance of more than 50% of all misfolded proteins (24). Apart from this considerable role in protein quality management, it has numerous regulatory functions, including roles in stress responses, metal homeostasis, biofilm formation, virulence, and persister cell formation (25). In line with this broad functionality, the Lon protease has a promiscuous substrate repertoire rather than a universal recognition motif. It recognizes either stably folded proteins with special recognition tags or unfolded polypeptides with accessible hydrophobic residues that are otherwise buried in the native structure (26). ClpP-type proteases also are important for the removal of misfolded proteins and for regulatory purposes. They are composed of proteolytic rings of ClpP subunits associated with rings

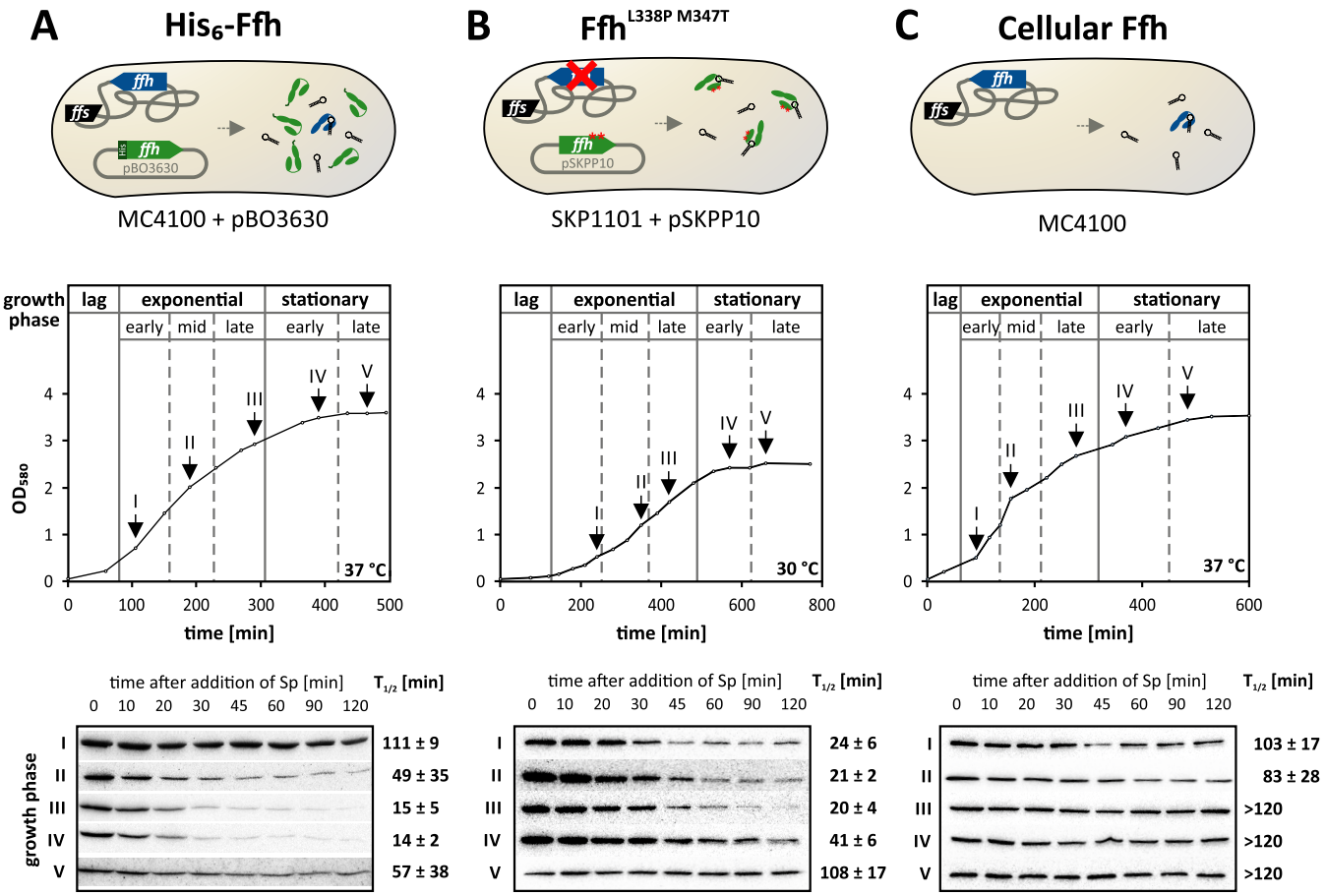

FIG 1 Stability of different Ffh variants at different growth phases. Protein stability was analyzed throughout all growth phases. Subcultures for half-life determination were taken at the indicated growth phases (I to V). Translation was stopped by the addition of 300 μg/ml spectinomycin (Sp) and samples were taken at the time points indicated. After SDS-PAGE, Western transfer, and immunodetection, protein half-lives ($t_{1/2}$) and standard deviations were calculated from three biological replicates. The *ffh* and *ffs* genes code for the Ffh protein and 4.5S RNA, respectively. (A) Plasmid-encoded His_6-Ffh (pBO3630) was induced by adding 50 ng/μl anhydrotetracycline hydrochloride (AHT) for 30 min in cultures grown at 37°C and detected by penta-His–HRP conjugate. (B) Half-lives of the plasmid-encoded temperature-sensitive $Ffh^{L338P\ M347T}$ variant (pSKPP10) were determined in *E. coli* SKP1101 at 30°C. (C) Stability of chromosomally encoded Ffh was analyzed at 37°C. Ffh and $Ffh^{L338P\ M347T}$ were detected by monoclonal anti-Ffh antibody.

of the ATPase subunits ClpX or ClpA, which are responsible for substrate recognition and delivery (27).

The substrates of all these proteases are difficult to predict and their identification requires experimentation, such as substrate-trapping approaches (28). In previous work, we found Ffh trapped with an inactive variant of the FtsH protease (29). The protein (derived from an expression plasmid from the ASKA collection) (30) was degraded both in an *E. coli* wild-type strain and *ftsH* mutant, suggesting that not FtsH but another protease was responsible for Ffh proteolysis. In this study, we set out to clarify which protease is responsible for Ffh degradation and which region of Ffh is recognized. We report that Ffh stability is differentially regulated and that Lon is the primary Ffh-degrading protease. We also show that the M domain of Ffh is necessary for degradation and that it induces synthetic lethality in the *lon* mutant. We conclude that the M domain is a multipurpose hub able to interact with various partners and thereby directing Ffh to different fates.

RESULTS

Plasmid-derived Ffh is subject to growth phase-dependent proteolysis. The previously reported half-life of overproduced free Ffh (20 min) was determined at a single time point in exponential phase (12). For a more comprehensive picture, we monitored Ffh stability along the entire growth curve (Fig. 1). Samples for stability

measurements were taken in early (I), mid (II), and late (III) exponential-growth phases, as well as in early (IV) and late (V) stationary-growth phases. To analyze the stability of plasmid-encoded His_6-Ffh, gene expression was induced by anhydrotetracycline hydrochloride (AHT) for 30 min prior to translation inhibition. The plasmid-derived $Ffh^{L338P\ M347T}$ variant with low RNA-binding capacity and the chromosome-encoded Ffh did not require external inducers. In all cases, translation was stopped by the addition of spectinomycin (Sp) and samples were taken and prepared for SDS-PAGE and Western transfer.

The half-life ($t_{1/2}$) of plasmid-derived His_6-Ffh produced in *E. coli* MC4100 cells grown at 37°C varied greatly with the growth phase (Fig. 1A). The protein was very stable in early exponential-growth phase ($t_{1/2}$ of almost 2 h), but rapidly degraded in late-exponential- and early-stationary-growth phase with half-lives around 15 min before stability increased again toward late stationary phase. These results are consistent with previous pulse-chase experiments showing half-lives of approximately 20 min in exponential-growth phase (12), but go beyond them in revealing growth-phase modulated turnover of the SRP protein.

Since several studies have suggested that the RNA-binding capacity of Ffh influences its stability (12, 31), we analyzed the growth-phase related stability of a temperature-sensitive Ffh variant carrying point mutations in the M domain that reduce the affinity to 4.5S RNA and render it more unstable than the wild-type protein (32). $Ffh^{L338P\ M347T}$ was constitutively expressed from a medium-copy-number plasmid in an *ffh* mutant strain viable at 30°C. The Ffh variant was indeed degraded much faster than wild-type His_6-Ffh during the early and mid phases of exponential growth but likewise stabilized toward stationary phase (Fig. 1B).

Finally, we assayed whether chromosomally encoded Ffh is subject to proteolysis over the entire growth range and found that it is barely degraded in early and mid-exponential-growth phases ($t_{1/2}$ of around 1.5 h), and fully stable with half-lives of more than 2 h in later growth phases (Fig. 1D). We conclude that Ffh is particularly prone to degradation when it is overabundant in the cell.

Lon is the primary protease responsible for Ffh degradation. Since the identity of the protease(s) responsible for Ffh degradation is not known, we monitored the stability of plasmid-derived His_6-Ffh throughout the growth curve in various protease-deficient *E. coli* strains and their corresponding parental strains. The growth phase-dependent degradation pattern described above for *E. coli* MC4100 (Fig. 1A and graphic representation in Fig. 2) was similar in all *E. coli* wild-type strains (MG1655, W3110, and BW25113) (see Fig. S1 in the supplemental material). As observed previously (29), Ffh is still degraded in the Δ*ftsH* strain, which grows poorly since the membrane-anchored FtsH protease is essential because of its role in LPS biosynthesis. The strain is viable only at low temperatures and in the presence of a suppressor mutation in the phospholipid biosynthesis pathway (23, 33). In the *hslUV* and *clpP* mutants, Ffh degradation resembled the wild-type pattern in being stabilized in early exponential (I) and late stationary (V) phase and being degraded in the intermediate growth phases (Fig. 2). These results indicate that the cytosolic HslUV and ClpAP or ClpXP proteases do not play a major role in Ffh turnover. In the *lon* deletion strain, however, Ffh was considerably stabilized in all tested growth phases. Even in mid-exponential phase (III), the half-life was around 1 h instead of 15 to 20 min in the wild-type (Fig. 1A). Since Ffh was not completely stable in the *lon* mutant, we used a strain lacking the nonessential cytosolic proteases Lon, ClpAP/XP, and HslUV because it is known that *E. coli* proteases share some of their substrates. Ffh was about 1.5- to 2-fold more stable in the triple mutant than in the Δ*lon* background alone (Fig. 2), demonstrating that Ffh degradation is primarily executed by the Lon protease and that ClpAP, ClpXP, and HslUV play a minor role as a backup system.

The amount of chromosome-encoded Ffh is modulated during bacterial growth. Having determined the growth phase-dependent half-lives of Ffh, we wondered whether its steady-state levels fluctuate during growth. First, the relative

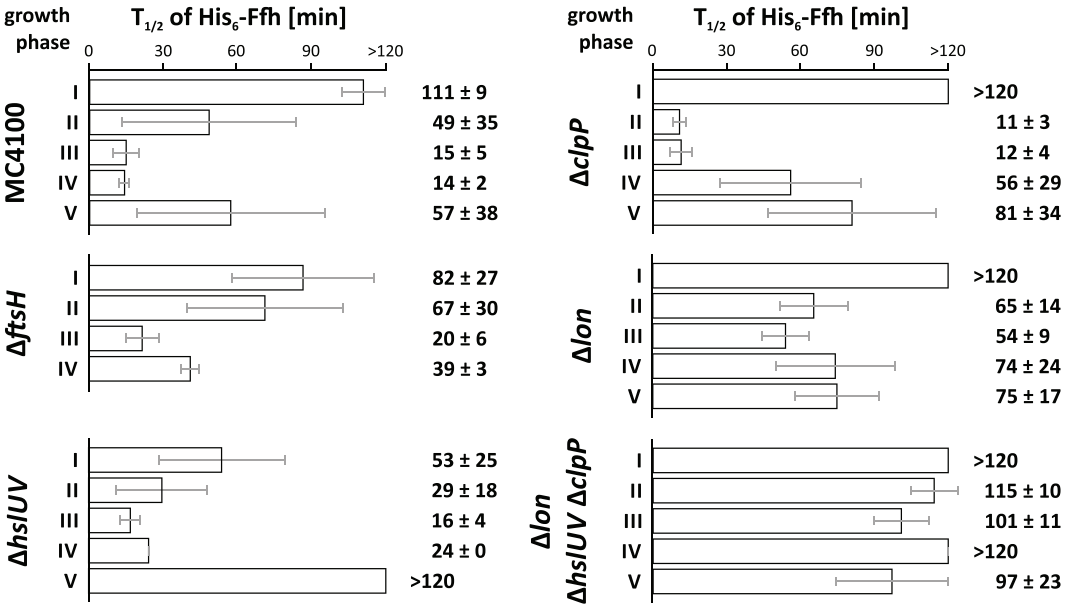

FIG 2 Stability of plasmid-derived His_6-Ffh in protease-deficient *E. coli* strains. The half-life of plasmid-derived His_6-Ffh in the wild-type MC4100 (data from Fig. 1A) and in the Δ*ftsH*, Δ*hslUV*, Δ*clpP*, Δ*lon*, and Δ*lon* Δ*hslUV* Δ*clpP* strains was measured as described in the legend to Fig. 1. Standard deviations derive from three biological replicates.

amounts of chromosomally encoded Lon and Ffh were compared in *E. coli* MC4100 (Fig. 3) from samples taken in growth phases I to V (Fig. 1A). Protein amounts measured by Western blotting were calculated relative to the amount in exponential-growth phase (I), which was set to 100%. The cellular amount of the Lon protease stayed almost constant throughout all growth phases (Fig. 3A). In contrast, the Ffh amount was highest during early exponential growth and then gradually decreased to about 30% in the subsequent growth phases (Fig. 3B). This results shows that the cellular Ffh levels are adjusted to the growth phase. In the Δ*lon* mutant, the Ffh amount decreased only to about 65%, consistent with the major contribution of the Lon protease to intracellular Ffh modulation.

The Lon-mediated depletion of Ffh levels was much more evident when His_6-Ffh was produced (Fig. 3C). Compared to endogenous Ffh, the His_6-Ffh levels were more than 20-fold higher in MC4100 and more than 30-fold higher in the Δ*lon* mutant in growth phase I. During growth, excess His_6-Ffh was rapidly removed in MC4100 and reached a final concentration only about 3-fold higher than endogenous Ffh in late stationary-growth phase (V). In contrast, degradation of His_6-Ffh in the *lon* mutant was much less efficient and left a 15-fold excess of His_6-Ffh compared to endogenous Ffh.

Overall, these results show that the cellular Ffh amount is highly dynamic and adjusted by regulated proteolysis. Overproduced SRP protein was most abundant (Fig. 3) and most stable (Fig. 1) in the beginning of exponential phase when growth starts to accelerate and the demand for membrane protein targeting is high. Rapid proteolysis at late exponential and early stationary phase with half-lives in the 15 min range depleted the His_6-Ffh concentration to almost physiological levels. Stabilization of the protein in late exponential phase (Fig. 1) is probably necessary to avoid reaching concentrations that are too low. Interestingly, Ffh levels were always reduced toward stationary phase, i.e., when protein biosynthesis slows down, regardless of whether Ffh was chromosome or plasmid encoded (Fig. 3B and C), suggesting that the cell closely monitors and balances the Ffh concentration in response to the physiological demand.

The M domain of Ffh is the target of the Lon protease. Next, we wanted to determine which Ffh region the Lon protease recognizes. The Ffh protein can be divided into two functional domains, the N-terminal NG domain and the C-terminal M domain. The methionine-rich M domain binds signal sequences of nascent proteins at

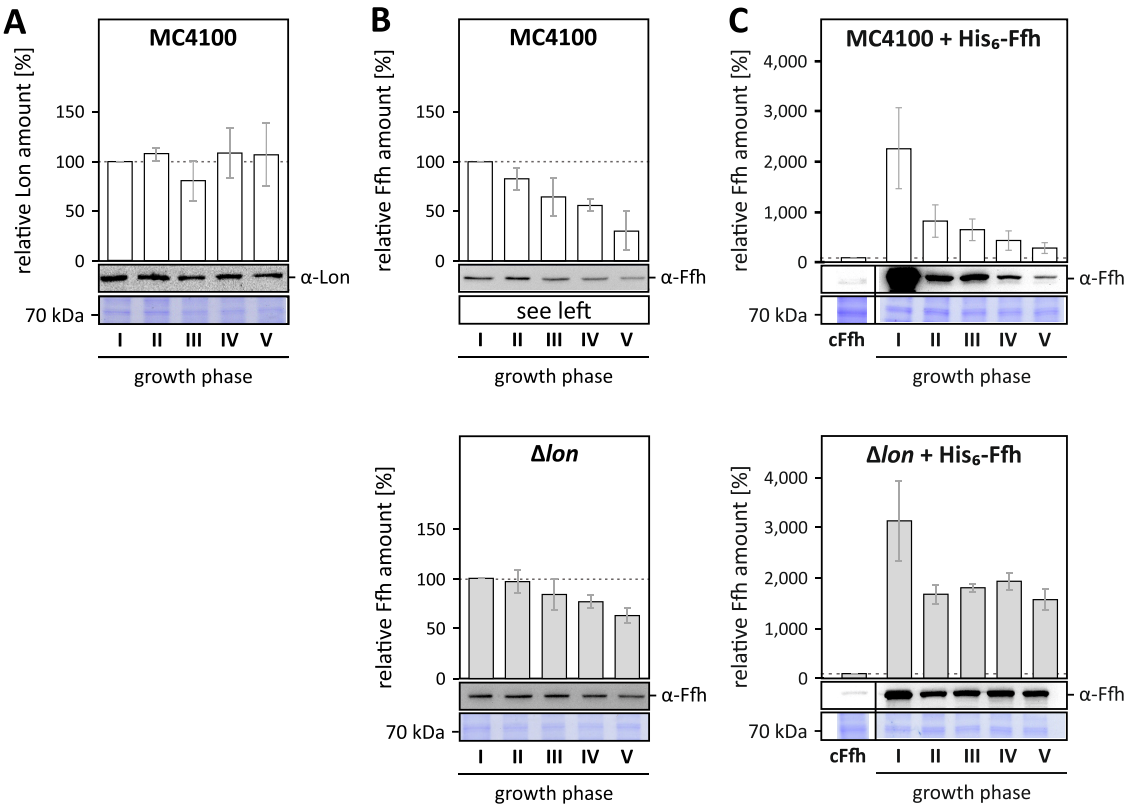

FIG 3 Cellular amounts of Lon and Ffh during growth. The relative protein amounts were analyzed by quantitative Western blot analysis. Samples were taken at defined time points of bacterial growth (I to V) as shown in Fig. 1. (A) The cellular Lon amount in *E. coli* MC4100 was immunologically detected with an anti-Lon antibody. (B) The cellular Ffh (cFfh) amount in MC4100 and Δ*lon* was determined by a monoclonal anti-Ffh antibody. (C) The expression of plasmid-encoded His_6-Ffh was induced by addition of 50 ng/μl AHT for 30 min and the protein was detected by a monoclonal anti-Ffh antibody. Quantification is based on three biological replicates and the samples of cellular Ffh or Lon in phase I were set to 100%. A section of a Coomassie-stained SDS gel at about 70 kDa is shown as loading control.

the ribosome and interacts with the 4.5S RNA (Fig. 4A), whereas the GTPase-harboring NG domain interacts with the membrane-anchored SRP receptor FtsY. We analyzed the stability of the isolated Ffh domains in *E. coli* strain MC4100 by *in vivo* degradation experiments at different growth phases (Fig. 4B). Each domain was produced as an N-terminally His_6-tagged variant from plasmids with an AHT-inducible promoter. His_6-NG was a completely stable protein with half-lives longer than 2 h (Fig. 4C). In contrast, His_6-M was prone to proteolysis and degraded under all conditions, with half-lives between 20 and 50 min (Fig. 4D). Like the full-length protein, the stability of the M domain was highest in phase I. Stabilization toward late stationary phase was not observed with the domain alone. Repeatedly, the protein was not detectable at all in this growth phase. Overall, the separation of Ffh into its two functional domains suggests that the M domain rather than the NG domain is responsible for proteolysis.

The *E. coli* M domain induces a lethal phenotype in the *lon* mutant. During our attempts to confirm that the Lon protease is responsible for proteolysis of the M domain, we made an unexpected observation. Despite repeated attempts, we were unable to transform plasmids expressing the M domain into the *lon* mutant. To further investigate this synthetic lethal phenotype, we determined the transformation frequencies of various Ffh constructs in *E. coli* wild type and the *lon* mutant.

All plasmids encoding the His_6-tagged variants of Ffh or the NG or M domains (Fig. 5A) were transformable into *E. coli* strain MC4100. Plating efficiencies were comparable for the empty vector control (His_6-EV) and the plasmid encoding the NG domain and about 2-fold lower for the plasmid encoding full-length Ffh (Fig. 5B). Colonies were also obtained with the M domain-encoding plasmid, although the transformation efficiency

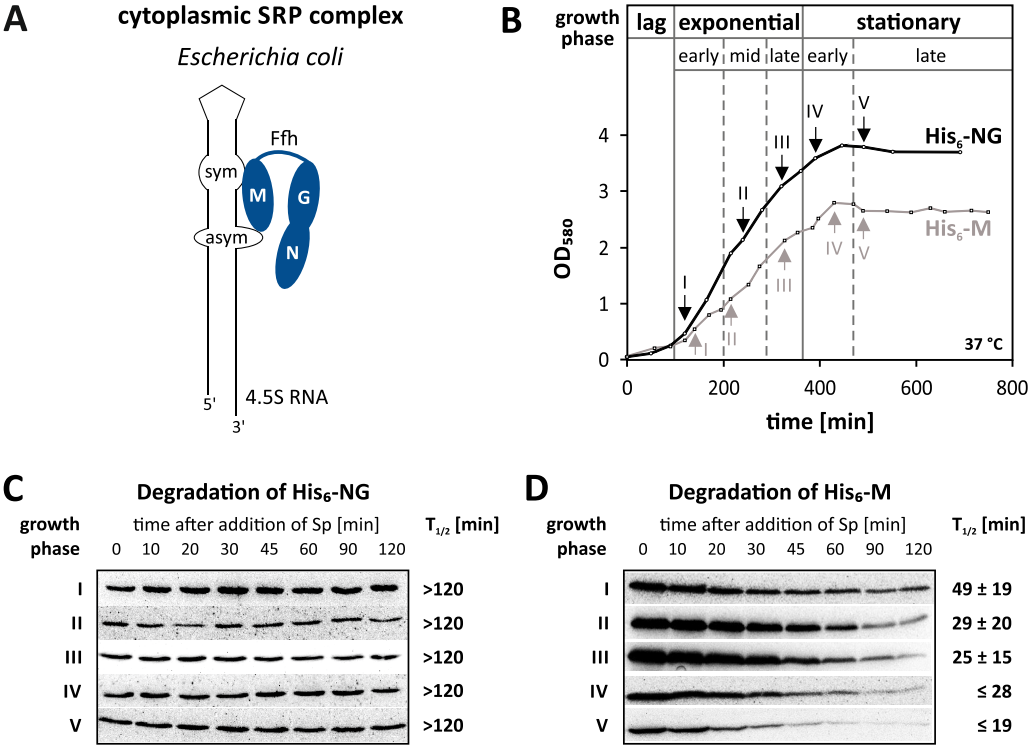

FIG 4 Stability of the NG and M domains of Ffh. (A) Schematic illustration of *E. coli* SRP composed of the Ffh protein and the 4.5S RNA. The N, G, and M domains from the N to C terminus are indicated; sym and asym in the 4.5S RNA denote the symmetric and asymmetric loop, respectively. (B) Growth curves of *E. coli* MC4100 producing plasmid-encoded His-tagged NG or M domains. Subcultures for half-life determination were taken at the indicated growth phases (I to V). The stability of the NG domain (C) and M domain (D) was determined by Western blotting as described for the His-tagged full-length protein in Fig. 1. Half-lives and standard deviations were calculated from at least three biological replicates except for samples IV and V in panel D, for which protein bands were not detectable in the late growth phases in several replicates.

was about 1,500 times lower than the empty vector. Microscopic inspection of the cell morphology of plasmid-carrying MC4100 cells in exponential- and stationary-growth phases revealed a normal appearance of bacteria with the empty vector or producing full-length Ffh or its NG domain (Fig. 5G). In contrast and indicative of severe growth defects, cells with the plasmid-encoded M domain were elongated in exponential phase and filamentous in stationary phase.

Transformation efficiencies in the Δ*lon* strain were generally about 3-fold lower than in MC4100 (Fig. 5C). Nonetheless, His_6-EV-, His_6-Ffh-, and the His_6-NG-encoding plasmids were easily transformable. In contrast, numerous attempts to transform the M domain-encoding plasmid into the *lon* mutant failed, suggesting synthetic lethality of the M domain in the absence of the Lon protease.

A single colony was obtained in one of the multiple transformation experiments of the M domain plasmid into the Δ*lon* strain. Sequencing of the insert of the plasmid from this clone provided insights into the region responsible for the lethal phenotype. The plasmid carried a large deletion covering the region for amino acids (aa) 388 to 453, in which the RNA-binding motif of the M domain (aa 382 to 407) is located. Apparently, the inactivated RNA-binding motif was able to reverse the lethality of the M domain in the *lon* mutant.

To investigate whether the lethality induced by the M domain can be blocked by the presence of additional N- or C-terminal domains that might induce conformational or functional changes of the M domain, we tested constructs of a bacterial one-hybrid system initially established as an approach to screen for protease inhibitors (34) and previously used to screen for proteolysis-resistant variants of the heat shock sigma factor RpoH (35). In this system, a gene or gene fragment of interest is flanked by the

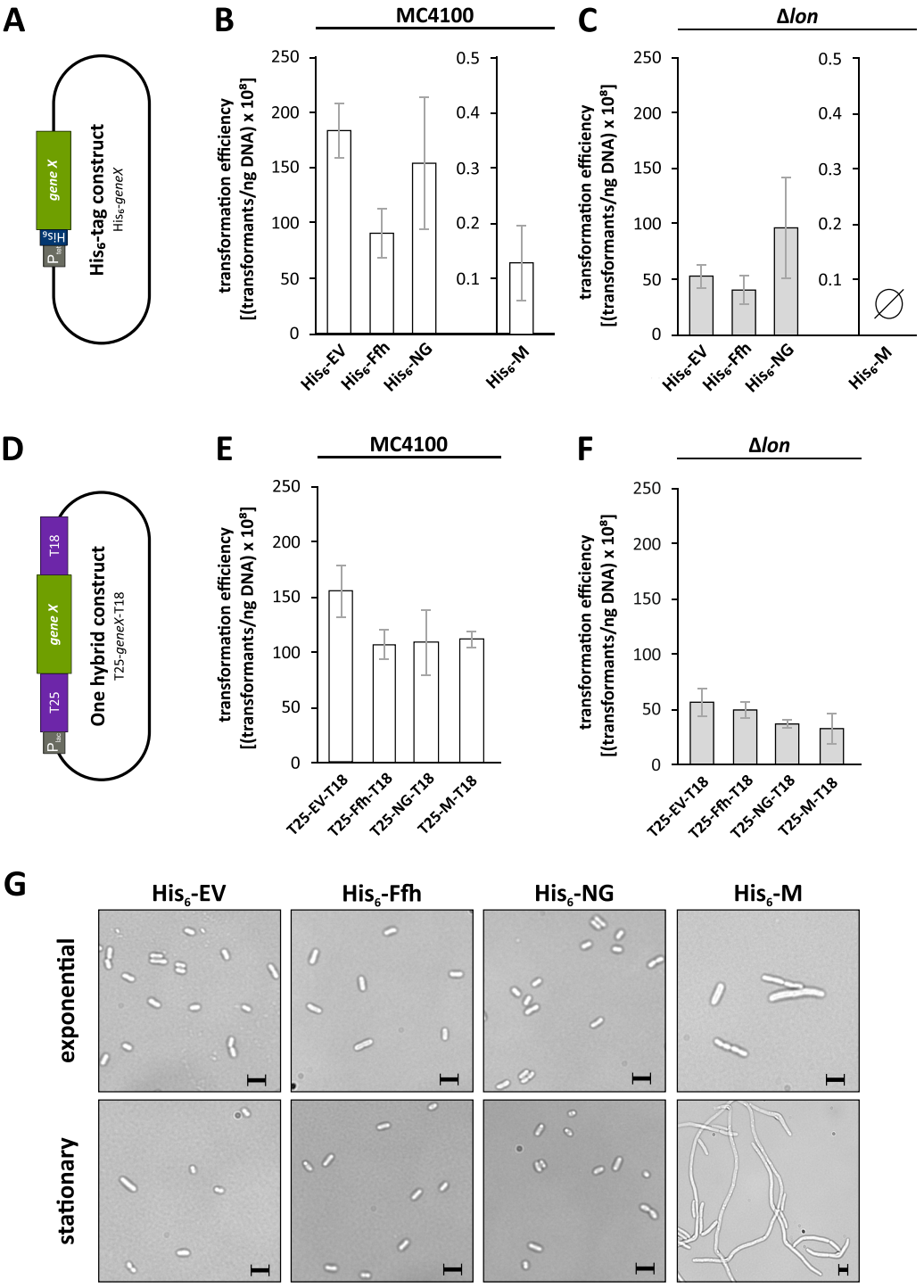

FIG 5 Transformation efficiencies of plasmid-encoded Ffh and its functional domains. Transformation efficiencies were determined for Ffh and its functional domains, NG or M domain, as His_6 tag constructs or one-hybrid constructs. (A) His_6 tag constructs encoding an N-terminal His_6 tag as well as the corresponding gene sequence (*geneX*) under the control of a tet promoter (P_{tet}). (B and C) Transformation efficiencies were determined for His_6 tag constructs in the *E. coli* MC4100 strain (B) and Δ*lon* mutant (C). (D) Plasmids of the one-hybrid constructs encoding the T25 and T18 domains of the adenylate cyclase *cyaA* from *B. pertussis* and the corresponding gene sequence was cloned between both domains under the control of a *lac* promoter (P_{lac}). Transformation efficiencies of the one-hybrid constructs were also determined in the *E. coli* MC4100 strain (E) and Δ*lon* mutant (F). (G) Light microscopy of *E. coli* MC4100 carrying His_6 tag constructs. Cells transformed with the empty vector (EV), plasmid-encoded Ffh, plasmid-encoded NG domain, or plasmid-encoded M domain were grown to exponential- or stationary-growth phase prior to light microscopy at 100-fold magnification. The scale bars correspond to 5 μm.

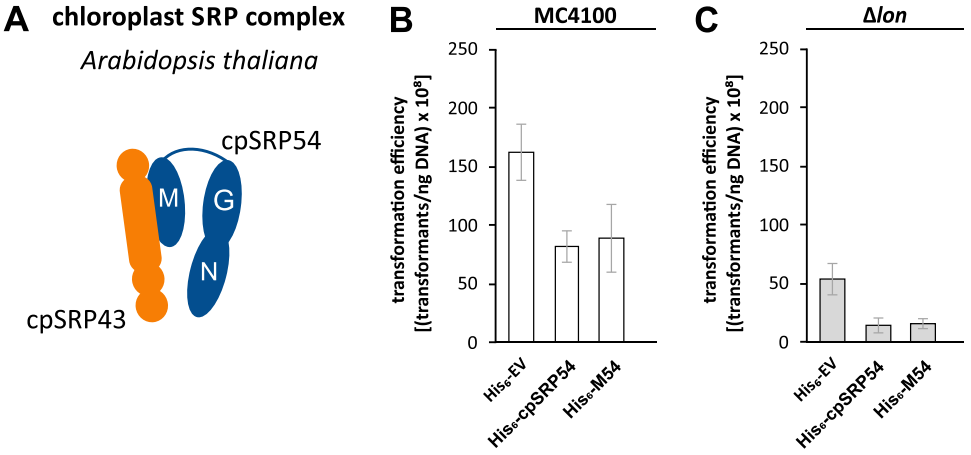

FIG 6 Transformation efficiencies of plasmid-encoded *Arabidopsis* cpSRP54 protein or its M domain into *E. coli* strain MC4100 or the Δ*lon* mutant. (A) The chloroplast SRP complex from *A. thaliana* consists of two protein components, the highly conserved cpSRP54 and the additional cpSRP43. (B and C) Transformation efficiencies are shown for plasmid-encoded His_6-tagged full-length cpSRP54 (His_6-cpSRP54) (B) or its M domain (His_6-M54) (C). The constructs were cloned as shown in Fig. 5A. For each construct and strain the corresponding empty vector (EV) was used as a control. Transformation efficiencies were calculated from three independent experiments.

open reading frames of the T25 and T18 domains of the adenylate cyclase from *Bordetella pertussis* (Fig. 5D). When the M domain was encoded in this context, the plasmid could be transformed with almost equal efficiency as the other plasmids into *E. coli* MC4100 (Fig. 5E). Interestingly, the T25-M domain-T18 fusion construct could also be transformed into the *lon* mutant almost as efficiently as the other constructs (Fig. 5F) and the cells were normal in length and morphology (data not shown).

To corroborate that an intact RNA-binding motif is responsible for the lethal phenotype in the *E. coli lon* mutant, we used the *Arabidopsis* cpSRP54 protein, a natural variant without RNA-binding capacity (see below). Instead of an RNA component, the M domain of cpSRP54 interacts with a protein partner called cpSRP43 (Fig. 6A). We determined the transformation efficiencies of plasmid-encoded His_6-cpSRP54 (the full-length protein) and His_6-M54 (the M domain of cpSRP54) in MC4100 and Δ*lon*. Plating efficiencies of both constructs into MC4100 were comparable to those of the full-length *E. coli* Ffh construct (Fig. 6B, compare with Fig. 5B). A remarkable difference was observed in the Δ*lon* strain (Fig. 6C). Here, it was possible to transform the His_6-M54 plasmid with equal efficiency as the plasmid coding for the full-length protein. This result further supports the hypothesis that an intact RNA-binding motif in the M domain induces the lethality in the *lon* mutant.

RNA-binding capacity is necessary for Ffh degradation. Our combined results suggested that the M domain is responsible for Ffh degradation and that it is toxic in the absence of the Lon protease when it has a functional RNA-binding region. To further address whether an intact RNA-binding motif is necessary for Lon-mediated degradation, we followed two strategies as follows: (i) we introduced point mutations into the RNA-binding region of *E. coli* Ffh and (ii) we used the *Arabidopsis* cpSRP54 protein, a natural variant without RNA-binding capacity.

For the first strategy, we introduced point mutations in *E. coli* Ffh leading to amino acid exchanges in S382, G405, and C406 (Fig. 7A and B). These residues are directly involved in RNA binding (36). The His_6-Ffh variants S382V or C406S had no influence on the growth phase-dependent degradation pattern in *E. coli* MC4100 (Fig. S2). These variants had short half-lives in the intermediate growth phases and were stable in early exponential and late stationary phase. The half-lives of the double mutant in phases II to IV were slightly higher than in the single mutants, but the overall pattern resembled that of the wild-type protein (Fig. 2). In contrast, exchanges at position G405 led to more stable proteins (Fig. S2), suggesting that Ffh residue G405 is involved in recognition by the Lon protease. We interpret these results cautiously because the G405

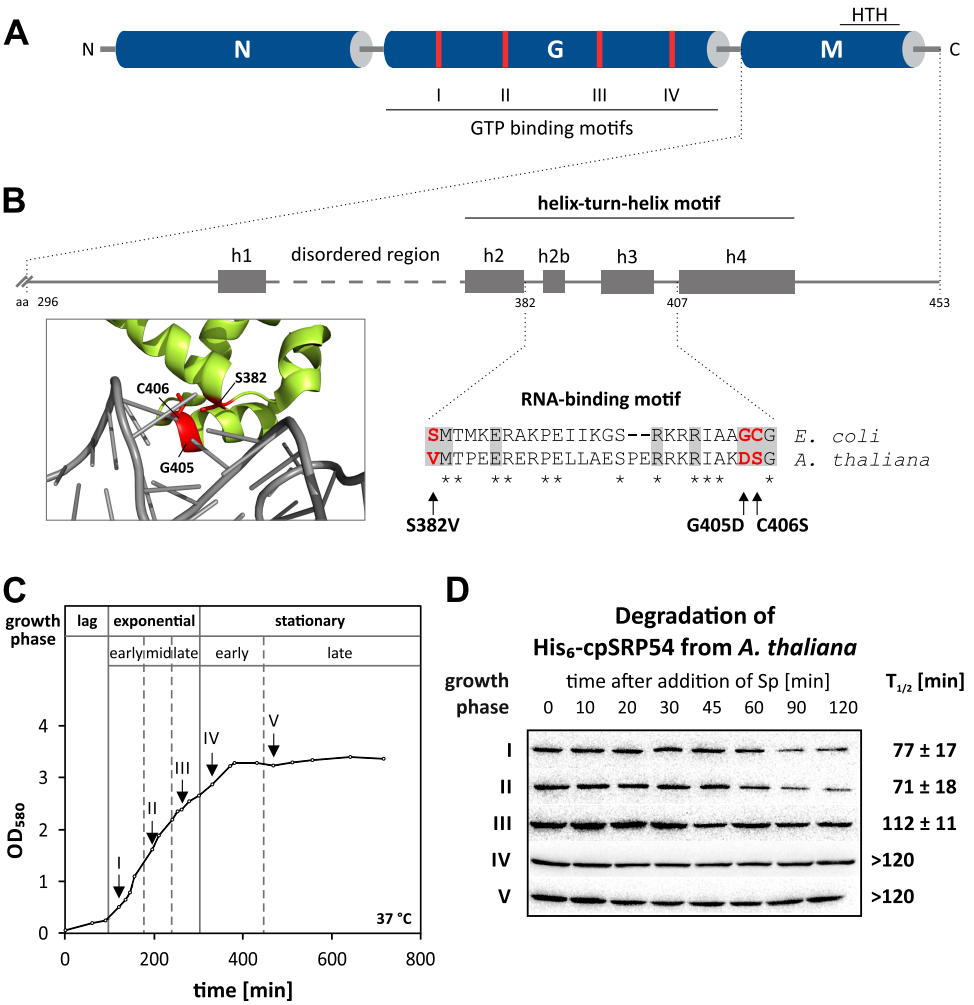

FIG 7 Point mutations in the M domain impact degradation of the SRP protein. (A) Domain arrangement of the *E. coli* Ffh protein. The G domain contains four conserved GTP-binding motifs (I, II, III, and IV). The helix-turn-helix motif (HTH) in the C-terminal M domain is responsible for 4.5S RNA-binding. (B) Schematic overview of the organization of the *E. coli* M domain (aa 296 to 453). The HTH consists of four helices. The RNA-binding motif is located between amino acids 382 to 407. Asterisks in the alignment mark conserved amino acids. The indicated point mutations S382V, G405D, and C406S (red) are responsible for the loss of RNA binding in cpSRP54 from *A. thaliana*. The protein model showing the RNA-binding of *E. coli* Ffh was generated based on the structural analysis (PDB ID: 2XXA) by Ataide et al. (63). (C and D) Stability of cpSRP54 from *A. thaliana* was determined by *in vivo* degradation experiments as described in Materials and Methods.

variants tended to be insoluble. Therefore, we employed an independent line of evidence to show an involvement of the RNA-binding region in Ffh turnover and exploited a natural Ffh variant without RNA-binding activity. The cpSRP protein from *A. thaliana* shows high sequence similarity to *E. coli* Ffh but lacks RNA-binding ability due to two amino acid substitutions in the RNA-binding domain where the SM---GXG motifs are exchanged to VM---DXG (Fig. 7B) (37). We found that cpSRP54 is a poor protease substrate in *E. coli* (Fig. 7C and D). It was degraded slowly in early growth phases (half-life between 70 and 80 min) and even more stable later on. Thus, the growth phase-dependent degradation as described for *E. coli* Ffh does not apply to chloroplast SRP54.

DISCUSSION

Although cotranslational delivery of inner membrane proteins is an essential process, *E. coli* tolerates large variations in SRP levels without dramatic effects on viability of the cell (14, 15). Nonetheless, the SRP amount in the cell must be calibrated because

severe depletion of either Ffh or the 4.5S RNA have profound effects on membrane protein homeostasis (16, 38). Our results show that the Lon protease balances the cellular Ffh levels and that the M domain is the target of proteolysis.

Interplay between the Lon and FtsH proteases. Our initial motivation to look into the proteolysis of Ffh was the recent finding that the protein was associated with an inactive FtsH variant in an *in vivo* substrate-trapping approach (29). It was therefore plausible to believe that FtsH is the protease responsible for the previously reported instability of free Ffh (12). Instead of FtsH, we report here that Lon is the primary protease for Ffh degradation. The HslUV and ClpXP/AP systems may join in as backup systems. Such substrate sharing with different preferences among the proteases is a well-established phenomenon. For example, the zinc-responsive transcription factor ZntR is degraded by Lon and ClpXP (39). The related copper efflux regulator CueR is primarily a Lon substrate but also moderately stabilized in the *clpP* mutant (40). Quality control pathways also heavily rely on substrate sharing, with the goal to remove aberrant and mislocalized proteins efficiently. For example, SsrA-tagged proteins, which are marked for degradation by the *trans*-translation system, are directed toward ClpXP, ClpAP, FtsH, and Lon (41–43).

It remains an open question why Ffh was found in a substrate-trapping approach with FtsH but not with Lon (29, 44). A possible explanation is the close connection between protein translocation and the heat shock response. In *E. coli*, regulation of the heat shock response depends on the sigma factor σ^{32} (RpoH), which associates with the RNA polymerase to initiate transcription of heat shock genes. Adjustment of the cellular RpoH level occurs at the transcriptional, translational, and posttranslational levels (45). The activity and abundance of RpoH is controlled by a homeostatic control mechanism, making sure that the sigma factor is inactive and eliminated when the demand for chaperones and proteases is low. This feedback process involves the chaperone systems DnaK/DnaJ/GrpE and GroEL/ES and the FtsH protease (46–48). In the absence of stress, the chaperones titrate the sigma factor away from the RNA polymerase and deliver it to FtsH. The proteases Lon, HslUV, and ClpXP can compensate for FtsH to some extent, providing another example of substrate sharing (49, 50). The accumulation of misfolded proteins under stress conditions occupies the chaperone machineries and releases RpoH for interaction with the RNA polymerase. The RpoH region responsible for targeting it to FtsH is region 2.1 and several point mutations in this region stabilize the sigma factor (35, 51). In the context of this study, it is interesting that this homeostatic control region in RpoH is able to interact with the M domain of Ffh. In turn, SRP directs the heat shock sigma factor to the inner membrane via the FtsY receptor for FtsH-dependent proteolysis (52, 53). Since approximately 50% of cellular RpoH is associated with the inner membrane (52), it is plausible that trapping of Ffh by FtsH was due to the protein-protein interaction network between Ffh, RpoH, and FtsH.

Based on this and previous studies, it emerges that the secretory pathway in *E. coli* is under close surveillance by the FtsH and Lon proteases. While Ffh is a substrate of Lon, several subunits of the Sec translocon are FtsH substrates (Fig. 8). The core Sec translocon formed by the membrane-spanning SecYEG complex mediates the insertion of inner membrane proteins and the transport of proteins across the inner membrane. Two proteins of the heterotrimeric complex are subjected to FtsH-mediated proteolysis. SecY is degraded when it is not assembled with SecE (29, 54, 55). SecE is another Sec protein stabilized in an *ftsH* mutant, whereas SecG is not (56). Among the auxiliary proteins, SecD was also found to be an FtsH substrate, whereas YidC was not (29).

Ffh proteolysis correlates with the cellular demand. Consistent with a previous report (12), we find that the half-life of over-overproduced Ffh is around 20 min in exponential growth phase. Tracking the half-life (Fig. 1) and steady-state level (Fig. 3) of Ffh over the entire growth curve provided interesting insights into the variability of Ffh proteolysis. The high concentration and stability of Ffh at the very early growth phase is counteracted thereafter by accelerated degradation, which removes excess Ffh until only slightly elevated levels have been reached. The increase in Ffh stability in

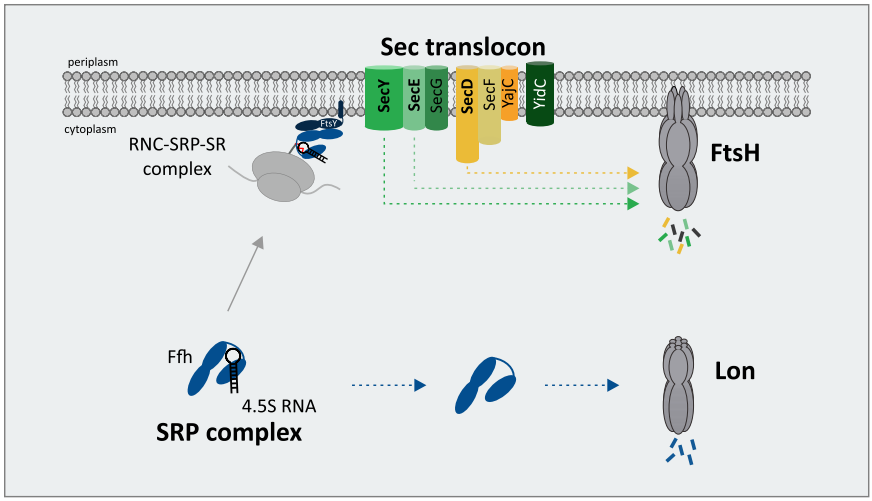

FIG 8 ATP-dependent proteolysis in protein translocation. The Sec translocon consists of the core proteins SecYEG and the ancillary proteins SecD, SecF, YajC, and YidC mediating protein translocation in or across the inner membrane. As part of protein quality control, the membrane proteins SecY, SecE, and SecD (in bold) are subjected to FtsH-dependent proteolysis. This study shows that the Lon protease controls the cotranslational protein-targeting pathway by degrading Ffh, the protein component of the signal recognition particle (SRP complex).

stationary phase might prevent it from dropping to levels too low for maintaining membrane homeostasis.

How is this growth-phase dependent process controlled? The most likely explanation already proposed by Jensen and Pedersen in 1994 is that Ffh is unstable when its concentration exceeds that of the 4.5S RNA (12). The principal function of the Lon protease, then, is to eliminate the pool of free, nonfunctional Ffh. Consistent with the previously reported 4-fold molar excess of 4.5S RNA to Ffh protein, which does not seem to fluctuate much through the curve (see Fig. S3 in the supplemental data), we found that the amount of overexpressed Ffh protein did not drop below a roughly 3-fold excess of the chromosomally provided Ffh. It thus appears that one function of the 4.5S RNA is to protect Ffh from proteolytic attack in order to maintain a sufficient amount of functional SRP in the cell.

Apart from Ffh, several other *E. coli* proteins are controlled by proteolysis to meet the acute cellular demand. For instance, LpxC, an essential enzyme catalyzing the first committed enzyme in lipopolysaccharide biosynthesis, is degraded by FtsH during slow growth when continued LPS production would be detrimental (57). YfgM, an ancillary SecYEG translocon subunit (58) and a negative regulator of the RcsB-dependent stress response, is degraded in stationary phase by FtsH to relieve inhibition of the stress response pathway and permit adaptation (59, 60). The reverse is true for the DNA replication inhibitor CspD. To adjust replication to the growth status, the Lon protease degrades CspD in fast-growing cells when rapid DNA replication is required, but leaves it intact in poorly growing cells (61). Hence, the growth phase-controlled proteolysis of Ffh adds a new example to the list of proteins that are removed when they are in excess and/or detrimental to growth under the prevailing condition.

The M domain is a multifunctional hub that determines the fate of Ffh. A separate analysis of the two subdomains of Ffh revealed that the M domain but not the NG domain is the target of proteolysis. This assigns yet another function to the M domain, which serves as a hub for various ligands and thereby routes Ffh toward different pathways. In total, the M domain has at least four potential interaction partners: the 4.5S RNA, the signal peptide of the nascent polypeptide, the heat shock sigma factor RpoH, and the Lon protease. Association with the 4.5S RNA and the signal peptide directs a membrane protein to the SRP receptor FtsY via interaction with the NG domain of Ffh. Apart from this canonical SRP function, the M domain is crucial for

two alternative pathways. As described above, an interaction with RpoH transports the transcription factor to the membrane where it is degraded by the membrane-anchored FtsH protease.

The new functionality discovered in this study is the role of the M domain in proteolytic Ffh turnover by the Lon protease. The M domain must be removed from the cell because it inhibits the expression of membrane proteins (17). A growth defect associated with the production of the M domain was clearly visible in MC4100 wild-type cells, which formed elongated filaments (Fig. 5G). The *lon* mutant did not even tolerate transformation of the M domain-encoding plasmid without inducer. This synthetic lethality was overcome in several ways: (i) when the RNA-binding region was destroyed in a mutant that we obtained fortuitously; (ii) when the M domain was blocked in a one-hybrid construct; (iii) when critical residues in the RNA-binding domain were exchanged; and (iv) when a natural non-RNA-binding Ffh homolog from *Arabidopsis* was used. These four lines of evidence support that Lon is the protease responsible for degradation of not only full-length Ffh but also the isolated M domain.

MATERIALS AND METHODS

Bacterial strains, plasmids, and media. All bacterial strains, vectors, and plasmids used in this study are listed in Tables S1, S2, and S3, respectively, in the supplemental data. Oligonucleotide sequences used for PCR and cloning are available upon request. *E. coli* cultures were grown at the indicated temperatures either on solid LB agar plates or in liquid LB medium supplemented with appropriate antibiotics if required (62).

Molecular biology methods. Molecular cloning of appropriate *ffh* fragments into expression vectors and site-directed mutagenesis were performed according to standard protocols (62). The correct sequences of plasmid inserts were validated by Sanger sequencing.

Determination of transformation efficiency. The plating efficiencies after transformation of empty vectors or plasmids encoding full-length Ffh, its NG domain or M domain, or cpSRP54 from *A. thaliana* were determined in *E. coli* MC4100 and Δ*lon* strains. For each construct, 100 ng of plasmid DNA and 100 μl of competent cells were used. After regeneration in 900 μl of liquid LB medium for 60 min at 37°C, cell suspensions were diluted from 10^0 to 10^{-4} and 100 μl of each dilution were plated on solid LB agar. Colonies were counted after incubation at 37°C for 24 h. To calculate transformation efficiencies ([transformants/bacterial titer]/nanogram of DNA), the bacterial titer of the competent MC4100 and Δ*lon* cells was determined after plating of 10^0 to 10^{-8} dilutions.

Light microscopy. *E. coli* cultures were inoculated at 37°C until exponential- and stationary-growth phases. Eight hundred microliters of a 1.5% agarose solution was applied on microscopy slides. The bacterial cultures were diluted to an optical density at 580 nm (OD_{580}) of about 0.5 and 10 μl were applied to the prepared slide and covered by a coverslip. Cells were inspected with an Olympus BX51 microscope at 100-fold magnification.

Western blot analysis and *in vivo* degradation experiments. To determine the stability of cellular Ffh or recombinant His_6-tagged proteins, samples were taken at different growth phases (Fig. 1A) and subjected to *in vivo* degradation experiments as described previously for other Lon substrates (44). Briefly, translation was blocked with spectinomycin (300 μg/ml) and aliquots were taken at different time points and frozen in liquid nitrogen. Cell pellets were resuspended in TE buffer (10 mM Tris-HCl [pH 8], 1 mM EDTA) according to the OD_{580} (100 μl TE buffer per OD_{580} = 1) and mixed with protein sample buffer with a final concentration of 2% SDS (wt/vol), 0.1% (wt/vol) bromophenol blue, 10% glycerol (vol/vol), 1% (vol/vol) β-mercaptoethanol, 50 mM Tris-HCl (pH 6.8). After incubation for 10 min at 95°C, proteins were separated by SDS-PAGE followed by Western transfer. His_6-tagged fusion proteins were detected with a penta-His–horseradish peroxidase (HRP) conjugate (Qiagen) at a dilution of 1:4,000. Monoclonal anti-Ffh (1:10,000) or anti-Lon (1:10,000) antibodies kindly provided by Hans-Georg Koch (Freiburg) and Axel Mogk (Heidelberg), respectively, were used for immunological detection of cellular Ffh or Lon. Goat anti-rabbit IgG (H+L)–HRP conjugate (1:3,000) served as secondary antibody, and chemiluminescence-based detection was carried out with Immobilon forte Western HRP substrate (Merck KGaA) and a ChemiImager Ready (Alpha Innotec). Protein half-lives were calculated with the help of the AlphaEaseFC software (version 4.0.0; Alpha Innotec).

SUPPLEMENTAL MATERIAL

Supplemental material is available online only.

SUPPLEMENTAL FILE 1, PDF file, 0.9 MB.

ACKNOWLEDGMENTS

We thank Hans-Georg Koch (Freiburg) and Axel Mogk (Heidelberg) for providing Ffh and Lon antisera, respectively. We thank Blanka Kutscher and Fitore Morina for experimental support and Hanno Boeddinghaus for help with figure preparation.

Financial support by grants from the German Research Foundation (DFG; SFB642,

GTP-, and ATP-dependent membrane processes; project A9 to F.N. and project A23 to D.S.) is gratefully acknowledged.

REFERENCES

1. Driessen AJ, Nouwen N. 2008. Protein translocation across the bacterial cytoplasmic membrane. Annu Rev Biochem 77:643–667. https://doi.org/10.1146/annurev.biochem.77.061606.160747.
2. Pool MR. 2005. Signal recognition particles in chloroplasts, bacteria, yeast and mammals. Mol Membr Biol 22:3–15. https://doi.org/10.1080/09687860400026348.
3. Akopian D, Shen K, Zhang X, Shan SO. 2013. Signal recognition particle: an essential protein-targeting machine. Annu Rev Biochem 82:693–721. https://doi.org/10.1146/annurev-biochem-072711-164732.
4. Steinberg R, Knüpffer L, Origi A, Asti R, Koch HG. 2018. Co-translational protein targeting in bacteria. FEMS Microbiol Lett 365:fny095. https://doi.org/10.1093/femsle/fny095.
5. Rosenblad MA, Samuelsson T. 2004. Identification of chloroplast signal recognition particle RNA genes. Plant Cell Physiol 45:1633–1639. https://doi.org/10.1093/pcp/pch185.
6. Träger C, Rosenblad MA, Ziehe D, Garcia-Petit C, Schrader L, Kock K, Vera Richter C, Klinkert B, Narberhaus F, Herrmann C, Hofmann E, Aronsson H, Schünemann D. 2012. Evolution from the prokaryotic to the higher plant chloroplast signal recognition particle: the signal recognition particle RNA Is conserved in plastids of a wide range of photosynthetic organisms. Plant Cell 24:4819–4836. https://doi.org/10.1105/tpc.112.102996.
7. Schuenemann D, Amin P, Hoffman NE. 1999. Functional divergence of the plastid and cytosolic forms of the 54-kDa subunit of signal recognition particle. Biochem Biophys Res Commun 254:253–258. https://doi.org/10.1006/bbrc.1998.9923.
8. Ziehe D, Dünschede B, Schünemann D. 2017. From bacteria to chloroplasts: evolution of the chloroplast SRP system. Biol Chem 398:653–661. https://doi.org/10.1515/hsz-2016-0292.
9. Hristou A, Gerlach I, Stolle DS, Neumann J, Bischoff A, Dünschede B, Nowaczyk MM, Zoschke R, Schünemann D. 2019. Ribosome-associated chloroplast SRP54 enables efficient cotranslational membrane insertion of key photosynthetic proteins. Plant Cell 31:2734–2750.
10. Ziehe D, Dünschede B, Zenker M, Funke S, Nowaczyk MM, Schünemann D. 2016. The chloroplast SRP systems of *Chaetosphaeridium globosum* and *Physcomitrella patens* as intermediates in the evolution of SRP-dependent protein transport in higher plants. PLoS One 11:e0166818. https://doi.org/10.1371/journal.pone.0166818.
11. Luirink J, von Heijne G, Houben E, de Gier JW. 2005. Biogenesis of inner membrane proteins in *Escherichia coli*. Annu Rev Microbiol 59:329–355. https://doi.org/10.1146/annurev.micro.59.030804.121246.
12. Jensen CG, Pedersen S. 1994. Concentrations of 4.5S RNA and Ffh protein in *Escherichia coli:* the stability of Ffh protein is dependent on the concentration of 4.5S RNA. J Bacteriol 176:7148–7154. https://doi.org/10.1128/JB.176.23.7148-7154.1994.
13. Dong H, Kirsebom LA, Nilsson L. 1996. Growth rate regulation of 4.5 S RNA and M1 RNA the catalytic subunit of *Escherichia coli* RNase P J Mol Biol 261:303–308. https://doi.org/10.1006/jmbi.1996.0461.
14. Ulbrandt ND, Newitt JA, Bernstein HD. 1997. The *E. coli* signal recognition particle is required for the insertion of a subset of inner membrane proteins. Cell 88:187–196. https://doi.org/10.1016/S0092-8674(00)81839-5.
15. Bernstein HD, Hyndman JB. 2001. Physiological basis for conservation of the signal recognition particle targeting pathway in *Escherichia coli*. J Bacteriol 183:2187–2197. https://doi.org/10.1128/JB.183.7.2187-2197.2001.
16. Wickström D, Wagner S, Baars L, Ytterberg AJ, Klepsch M, van Wijk KJ, Luirink J, de Gier JW. 2011. Consequences of depletion of the signal recognition particle in *Escherichia coli*. J Biol Chem 286:4598–4609. https://doi.org/10.1074/jbc.M109.081935.
17. Yosef I, Bochkareva ES, Bibi E. 2010. *Escherichia coli* SRP, its protein subunit Ffh, and the Ffh M domain are able to selectively limit membrane protein expression when overexpressed. mBio 1:e00020-10. https://doi.org/10.1128/mBio.00020-10.
18. Bittner LM, Arends J, Narberhaus F. 2016. ATP-dependent proteases in bacteria. Biopolymers 105:505–517. https://doi.org/10.1002/bip.22831.
19. Baker TA, Sauer RT. 2006. ATP-dependent proteases of bacteria: recognition logic and operating principles. Trends Biochem Sci 31:647–653. https://doi.org/10.1016/j.tibs.2006.10.006.
20. Mahmoud SA, Chien P. 2018. Regulated proteolysis in bacteria. Annu Rev Biochem 87:677–696. https://doi.org/10.1146/annurev-biochem-062917-012848.
21. Gur E, Biran D, Ron EZ. 2011. Regulated proteolysis in Gram-negative bacteria—how and when? Nat Rev Microbiol 9:839–848. https://doi.org/10.1038/nrmicro2669.
22. Langklotz S, Baumann U, Narberhaus F. 2012. Structure and function of the bacterial AAA protease FtsH. Biochim Biophys Acta 1823:40–48. https://doi.org/10.1016/j.bbamcr.2011.08.015.
23. Ogura T, Inoue K, Tatsuta T, Suzaki T, Karata K, Young K, Su LH, Fierke CA, Jackman JE, Raetz CRH, Coleman J, Tomoyasu T, Matsuzawa H. 1999. Balanced biosynthesis of major membrane components through regulated degradation of the committed enzyme of lipid A biosynthesis by the AAA protease FtsH (HflB) in *Escherichia coli*. Mol Microbiol 31:833–844. https://doi.org/10.1046/j.1365-2958.1999.01221.x.
24. Chung CH, Goldberg AL. 1981. The product of the *lon* (*capR*) gene in *Escherichia coli* is the ATP-dependent protease, protease La. Proc Natl Acad Sci U S A 78:4931–4935. https://doi.org/10.1073/pnas.78.8.4931.
25. Gur E. 2013. The Lon AAA+ protease. Subcell Biochem 66:35–51. https://doi.org/10.1007/978-94-007-5940-4_2.
26. Gur E, Sauer RT. 2008. Recognition of misfolded proteins by Lon, a AAA(+) protease. Genes Dev 22:2267–2277. https://doi.org/10.1101/gad.1670908.
27. Kress W, Maglica Z, Weber-Ban E. 2009. Clp chaperone-proteases: structure and function. Res Microbiol 160:618–628. https://doi.org/10.1016/j.resmic.2009.08.006.
28. Rei Liao JY, van Wijk KJ. 2019. Discovery of AAA+ protease substrates through trapping approaches. Trends Biochem Sci 44:528–545. https://doi.org/10.1016/j.tibs.2018.12.006.
29. Arends J, Thomanek N, Kuhlmann K, Marcus K, Narberhaus F. 2016. *In vivo* trapping of FtsH substrates by label-free quantitative proteomics. Proteomics 16:3161–3172. https://doi.org/10.1002/pmic.201600316.
30. Kitagawa M, Ara T, Arifuzzaman M, Ioka-Nakamichi T, Inamoto E, Toyonaga H, Mori H. 2005. Complete set of ORF clones of *Escherichia coli* ASKA library (a complete set of *E. coli* K-12 ORF archive): unique resources for biological research. DNA Res 12:291–299.
31. Zheng N, Gierasch LM. 1997. Domain interactions in *E. coli* SRP: stabilization of M domain by RNA is required for effective signal sequence modulation of NG domain. Mol Cell 1:79–87. https://doi.org/10.1016/S1097-2765(00)80009-X.
32. Park SK, Jiang F, Dalbey RE, Phillips GJ. 2002. Functional analysis of the signal recognition particle in *Escherichia coli* by characterization of a temperature-sensitive *ffh* mutant. J Bacteriol 184:2642–2653. https://doi.org/10.1128/JB.184.10.2642-2653.2002.
33. Führer F, Langklotz S, Narberhaus F. 2006. The C-terminal end of LpxC is required for degradation by the FtsH protease. Mol Microbiol 59:1025–1036. https://doi.org/10.1111/j.1365-2958.2005.04994.x.
34. Dautin N, Karimova G, Ullmann A, Ladant D. 2000. Sensitive genetic screen for protease activity based on a cyclic AMP signaling cascade in *Escherichia coli*. J Bacteriol 182:7060–7066. https://doi.org/10.1128/JB.182.24.7060-7066.2000.
35. Obrist M, Narberhaus F. 2005. Identification of a turnover element in region 2.1 of *Escherichia coli* sigma32 by a bacterial one-hybrid approach. J Bacteriol 187:3807–3813. https://doi.org/10.1128/JB.187.11.3807-3813.2005.
36. Batey RT, Rambo RP, Lucast L, Rha B, Doudna JA. 2000. Crystal structure of the ribonucleoprotein core of the signal recognition particle. Science 287:1232–1239. https://doi.org/10.1126/science.287.5456.1232.
37. Richter CV, Träger C, Schünemann D. 2008. Evolutionary substitution of two amino acids in chloroplast SRP54 of higher plants cause its inability to bind SRP RNA. FEBS Lett 582:3223–3229. https://doi.org/10.1016/j.febslet.2008.08.014.
38. Jensen CG, Brown S, Pedersen S. 1994. Effect of 4.5S RNA depletion on *Escherichia coli* protein synthesis and secretion. J Bacteriol 176:2502–2506. https://doi.org/10.1128/JB.176.9.2502-2506.1994.
39. Pruteanu M, Neher SB, Baker TA. 2007. Ligand-controlled proteolysis of the *Escherichia coli* transcriptional regulator ZntR. J Bacteriol 189:3017–3025. https://doi.org/10.1128/JB.01531-06.

40. Bittner LM, Kraus A, Schäkermann S, Narberhaus F. 2017. The copper efflux regulator CueR is subject to ATP-dependent proteolysis in *Escherichia coli*. Front Mol Biosci 4:9.
41. Gottesman S, Roche E, Zhou YN, Sauer RT. 1998. The ClpXP and ClpAP proteases degrade proteins with carboxy-terminal peptide tails added by the SsrA-tagging sytem. Genes Dev 12:1338–1347. https://doi.org/10.1101/gad.12.9.1338.
42. Herman C, Thévenet D, Bouloc P, Walker GC, D'Ari R. 1998. Degradation of carboxy-terminal-tagged cytoplasmic proteins by the *Escherichia coli* proease HflB (FtsH). Genes Dev 12:1348–1355. https://doi.org/10.1101/gad.12.9.1348.
43. Choy JS, Aung LL, Karzai AW. 2007. Lon protease degrades transfer-messenger RNA-tagged proteins. J Bacteriol 189:6564–6571. https://doi.org/10.1128/JB.00860-07.
44. Arends J, Griego M, Thomanek N, Lindemann C, Kutscher B, Meyer HE, Narberhaus F. 2018. An integrated proteomic approach uncovers novel substrates and functions of the Lon protease in *Escherichia coli*. Proteomics 18:e1800080.
45. Morita MT, Tanaka Y, Kodama TS, Kyogoku Y, Yanagi H, Yura T. 1999. Translational induction of heat shock transcription factor σ^{32}: evidence for a built-in RNA thermosensor. Genes Dev 13:655–665. https://doi.org/10.1101/gad.13.6.655.
46. Gamer J, Multhaup G, Tomoyasu T, McCarty JS, Rüdiger S, Schönfeld HJ, Schirra C, Bujard H, Bukau B. 1996. A cycle of binding and release of the DnaK, DnaJ and GrpE chaperones regulates activity of the *Escherichia coli* heat shock transcription factor σ^{32}. EMBO J 15:607–617. https://doi.org/10.1002/j.1460-2075.1996.tb00393.x.
47. Guisbert E, Herman C, Lu CZ, Gross CA. 2004. A chaperone network controls the heat shock response in *E. coli*. Genes Dev 18:2812–2821. https://doi.org/10.1101/gad.1219204.
48. Liberek K, Galitski TP, Zylicz M, Georgopoulos C. 1992. The DnaK chaperone modulates the heat shock response of *Escherichia coli* by binding to the σ^{32} transcription factor. Proc Natl Acad Sci U S A 89:3516–3520. https://doi.org/10.1073/pnas.89.8.3516.
49. Kanemori M, Nishihara K, Yanagi H, Yura T. 1997. Synergistic roles of HslVU and other ATP-dependent proteases in controlling in vivo turnover of σ^{32} and abnormal proteins in *Escherichia coli*. J Bacteriol 179:7219–7225. https://doi.org/10.1128/JB.179.23.7219-7225.1997.
50. Tomoyasu T, Gamer J, Bukau B, Kanemori M, Mori H, Rutman AJ, Oppenheim AB, Yura T, Yamanaka K, Niki H, Hiraga S, Ogura T. 1995. *Escherichia coli* FtsH is a membrane bound, ATP-dependent protease which degrades the heat-shock transcription factor σ^{32}. EMBO J 14:2551–2560. https://doi.org/10.1002/j.1460-2075.1995.tb07253.x.
51. Horikoshi M, Yura T, Tsuchimoto S, Fukumori Y, Kanemori M. 2004. Conserved region 2.1 of *Escherichia coli* heat shock transcription factor σ^{32} is required for modulating both metabolic stability and transcriptional activity. J Bacteriol 186:7474–7480. https://doi.org/10.1128/JB.186.22.7474-7480.2004.
52. Lim B, Miyazaki R, Neher S, Siegele DA, Ito K, Walter P, Akiyama Y, Yura T, Gross CA. 2013. Heat shock transcription factor sigma32 co-opts the signal recognition particle to regulate protein homeostasis in *E. coli*. PLoS Biol 11:e1001735. https://doi.org/10.1371/journal.pbio.1001735.
53. Miyazaki R, Yura T, Suzuki T, Dohmae N, Mori H, Akiyama Y. 2016. A novel SRP recognition sequence in the homeostatic control region of heat shock transcription factor sigma32. Sci Rep 6:24147. https://doi.org/10.1038/srep24147.
54. Kihara A, Akiyama Y, Ito K. 1995. FtsH is required for proteolytic elimination of uncomplexed forms of SecY, an essential protein translocase subunit. Proc Natl Acad Sci U S A 92:4532–4536. https://doi.org/10.1073/pnas.92.10.4532.
55. Akiyama Y, Kihara A, Tokuda H, Ito K. 1996. FtsH (HflB) is an ATP-dependent protease selectively acting on SecY and some other membrane proteins. J Biol Chem 271:31196–31201. https://doi.org/10.1074/jbc.271.49.31196.
56. van Stelten J, Silva F, Belin D, Silhavy TJ. 2009. Effects of antibiotics and a proto-oncogene homolog on destruction of protein translocator SecY. Science 325:753–756. https://doi.org/10.1126/science.1172221.
57. Schäkermann M, Langklotz S, Narberhaus F. 2013. FtsH-mediated coordination of lipopolysaccharide biosynthesis in *Escherichia coli* correlates with the growth rate and the alarmone (p)ppGpp. J Bacteriol 195:1912–1919. https://doi.org/10.1128/JB.02134-12.
58. Götzke H, Palombo I, Muheim C, Perrody E, Genevaux P, Kudva R, Müller M, Daley DO. 2014. YfgM is an ancillary subunit of the SecYEG translocon in *Escherichia coli*. J Biol Chem 289:19089–19097. https://doi.org/10.1074/jbc.M113.541672.
59. Bittner LM, Westphal K, Narberhaus F. 2015. Conditional proteolysis of the membrane protein YfgM by the FtsH protease depends on a novel N-terminal degron. J Biol Chem 290:19367–19378. https://doi.org/10.1074/jbc.M115.648550.
60. Westphal K, Langklotz S, Thomanek N, Narberhaus F. 2012. A trapping approach reveals novel substrates and physiological functions of the essential protease FtsH in *Escherichia coli*. J Biol Chem 287:42962–42971. https://doi.org/10.1074/jbc.M112.388470.
61. Langklotz S, Narberhaus F. 2011. The *Escherichia coli* replication inhibitor CspD is subject to growth-regulated degradation by the Lon protease. Mol Microbiol 80:1313–1325. https://doi.org/10.1111/j.1365-2958.2011.07646.x.
62. Sambrook J, Russell DW. 2001. Molecular cloning: a laboratory manual, 3rd ed. Cold Spring Harbor Laboratory Press, Cold Spring Harbor, New York.
63. Ataide SF, Schmitz N, Shen K, Ke A, Shan SO, Doudna JA, Ban N. 2011. The crystal structure of the signal recognition particle in complex with its receptor. Science 331:881–886. https://doi.org/10.1126/science.1196473.